



Writing of a Bragg Grating on a D-shaped Optical Fiber Using the KrF Excimer Laser

Shaymaa R. Mohammed⁽¹⁾ Rong Z. Chen⁽²⁾ Khalil I. Hajim⁽¹⁾ and Kevin P. Chen⁽²⁾

(1) *Institute of laser for postgraduate studies, University of Baghdad, Baghdad, Iraq.*

(2) *Department of Electrical and Computer Engineering, Swanson School of Engineering University of Pittsburgh, Pittsburgh, PA, USA.*

(Received 7 July 2014; accepted 26 October 2014)

Abstract: Fiber Bragg Grating has many advantages where it can be used as a temperature sensor, pressure sensor or even as a refractive index sensor. Designing each of this fiber Bragg grating sensors should include some requirements. Fiber Bragg grating refractive index sensor is a very important application. In order to increase the sensing ability of fiber Bragg gratings, many methods were followed. In our proposed work, the fiber Bragg grating was written in a D-shaped optical fiber by using a phase mask method with KrF excimer. The resultant fiber Bragg grating has a high reflectivity 99.99% with a Bragg wavelength of 1551.2 nm as a best result obtained from a phase mask with a grating period of 1057 nm. In this work it was found that the rotation of the core of the D-shaped optical fiber that faces the phase mask is very important in determining the quality of written fiber Bragg grating.

Introduction

Fiber Bragg grating (FBG) sensors are based on the change of the refractive index in the core of the optical fiber. FBGs have many advantages compared to other types of optical sensors where the information is obtained directly by detecting the wavelength shift due to the measurand (simple signal processing), FBGs can be written directly into the fiber core (easy to fabricate and mass production available at low costs) [1,2].

Hill et al., 1978 was the first who wrote a photoinduced grating on optical fiber core by the interference of counter propagating beams of argon laser [3]. A. Swanton et al., 1996 used the phase mask method to write a uniform photorefractive fiber Bragg gratings [4]. To enhance the written FBGs, high pressure Hydrogen gas was loaded into optical fibers to increase the UV photosensitivity [5,6].

A novel approach of designing a chemosensor based on cladding etched Bragg was reported by Zhou et al., 2004 where the sensitivity of the fiber Bragg grating to the surrounding medium refractive index was increased by HF etching. The measured sensitivity was 0.02nm/% for different sugar solution concentrations [7].

The presented work is concerned with the writing of Bragg gratings on a D-shaped optical fiber by a phase mask method.

The single mode D-shaped optical fiber is very useful in designing the refractive index sensor like chemical and biosensors because it is more flexible and less susceptible to break even chemically etching the cladding down to the core.

Theoretical Background

Contradirectional Coupled Mode Theory

In our Fiber Bragg Grating case the theory of contradirectional coupling from coupled

mode theory is considered as shown in Figure 1. Here mode a is forward propagating and mode b is backward propagating [8]. This is corresponding to $\beta_a > 0$ and $\beta_b < 0$

$$\delta = (\beta_a - \beta_b) = 2\pi n_{eff} \left(\frac{1}{\lambda_{inc}} - \frac{1}{\lambda_{Bragg}} \right) \quad (1)$$

where n_{eff} is the effective refractive index.

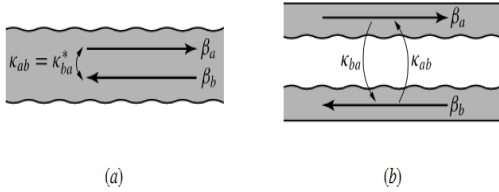


Fig. (1): Coupling between two modes propagating in opposite directions (a) in the same waveguide (b) in two parallel waveguide [8].

The coupling equations are

$$\frac{d\tilde{A}}{dz} = i\kappa_{ab}\tilde{B}e^{i2\delta z}, \quad (2)$$

$$-\frac{d\tilde{B}}{dz} = i\kappa_{ba}\tilde{A}e^{-i2\delta z}, \quad (3)$$

Where $\kappa_{ab} = -\kappa_{ba}$. These equations are solved as boundary conditions of $\tilde{A}(0)$ at one end and $\tilde{B}(l)$ at other end to find the values of $\tilde{A}(z)$ and $\tilde{B}(z)$ at any location z between two ends. So the general solution can be expressed in the following matrix form [8]:

$$\begin{pmatrix} \tilde{A}(z) \\ \tilde{B}(z) \end{pmatrix} = R(z; 0; l) \begin{pmatrix} \tilde{A}(0) \\ \tilde{B}(l) \end{pmatrix}, \quad (4)$$

where:

$$R(z; 0, l) = \begin{bmatrix} \frac{\alpha_c \cosh \alpha_c(l-z) + i\delta \sinh \alpha_c(l-z)}{\alpha_c \cosh \alpha_c l + i\delta \sinh \alpha_c l} e^{i\delta z} & \frac{i\kappa_{ab} \sinh \alpha_c z}{\alpha_c \cosh \alpha_c l + i\delta \sinh \alpha_c l} e^{i\delta(z+l)} \\ \frac{i\kappa_{ba} \sinh \alpha_c(l-z)}{\alpha_c \cosh \alpha_c l + i\delta \sinh \alpha_c l} e^{-i\delta z} & \frac{\alpha_c \cosh \alpha_c z + i\delta \sinh \alpha_c z}{\alpha_c \cosh \alpha_c l + i\delta \sinh \alpha_c l} e^{-i\delta(z-l)} \end{bmatrix} \quad (5)$$

where:

$$\alpha_c = (\kappa_{ab}\kappa_{ba} - \delta^2)^{1/2} \quad (6)$$

Under a simple case consideration where here if the power is launched only into mode at $z=0$, the boundary values are $\tilde{A}(0) \neq 0$ and $\tilde{B}(l) = 0$ by applying these conditions to (4), it found that [8]:

$$\tilde{A}(z) = \tilde{A}(0) \frac{\alpha_c \cosh \alpha_c(l-z) + i\delta \sinh \alpha_c(l-z)}{\alpha_c \cosh \alpha_c l + i\delta \sinh \alpha_c l} e^{i\delta z} \quad (7)$$

$$\tilde{B}(z) = \tilde{A}(0) \frac{i\kappa_{ba} \sinh \alpha_c(l-z)}{\alpha_c \cosh \alpha_c l + i\delta \sinh \alpha_c l} e^{-i\delta z} \quad (8)$$

In this case, contradirectional coupling can be used as reflection of field amplitude $\tilde{A}(0)$ at $z=0$ with reflection coefficient:

$$r = |r|e^{i\varphi_{DBR}} = \frac{\tilde{B}(0)}{\tilde{A}(0)} = \frac{i\kappa_{ba} \sinh \alpha_c l}{\alpha_c \cosh \alpha_c l + i\delta \sinh \alpha_c l} \quad (9)$$

Phase Mask Method

The easier inscription of fiber grating was made by the phase mask which is a component of interferometer. Phase Mask is a transmission grating etched in a silica plate. The most important properties of this type of the phase mask are the grooves etched into a UV – transmitting silica mask plate and etch depth and their mark – space ratio are carefully controlled. The operation is based on the diffraction of an incident UV beam into several orders, $M = 0, \pm 1, \pm 2, \dots$ as shown in Figure 2 [9],

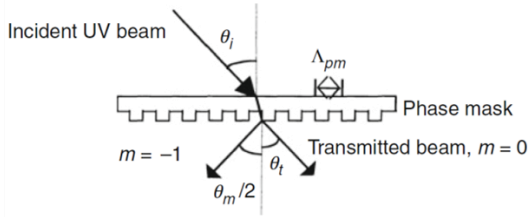


Fig. (2): A schematic of the diffraction of an incident beam from a phase mask [9].

The general diffraction equation is satisfied by the incident and diffracted orders with the phase mask period Λ_{pm} [9],

$$\Lambda_{pm} = \frac{m\lambda_{uv}}{\left(\sin\left(\frac{\theta_m}{2}\right) - \sin\theta_i\right)} \quad (10)$$

Where λ_{uv} is the incident UV laser wavelength θ_i is the angle of the incident UV beam and $\theta_m/2$ is the angle of the diffraction of order m . If $\frac{\lambda_{uv}}{2} \leq \Lambda_{pm} \leq \lambda_{uv}$, then the incident wave is diffracted into a single order ($m = -1$) and the rest of the power is transmitted at ($m = 0$). With UV radiation at normal incidence $\theta_i = 0$ the diffracted wave is split into three orders $m=0$ and $m=\pm 1$ as shown in Figure 3.

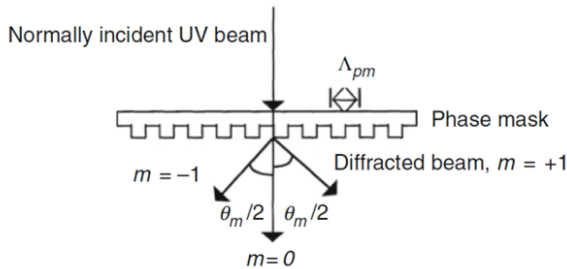


Fig. (3): Normally incident UV beam diffracted into two ± 1 orders. The remnant radiation exits the phase-mask in the zero order ($m = 0$) [9].

The two beams of orders $m = +1$ and $m = -1$ are then brought together by a two parallel mirrors and interfere producing an interference pattern at the fiber. This interference pattern has a period Λ_g related to the diffraction angle [9],

$$\Lambda_g = \frac{\lambda_{uv}}{2 \sin\left(\frac{\theta_m}{2}\right)} = \frac{\Lambda_{pm}}{2} \quad (11)$$

Tools and Methods

The procedure of writing a Bragg grating on a D-shaped optical fiber consists mainly of 2 stages. The first stage is soaking of D-shaped

optical fiber into H_2 chamber under high pressure. The second stage is writing the Bragg grating into the core of the fiber.

First stage: Soaking of the optical fiber into H_2 ,

The fiber employed in this work is a D-shaped fiber with core refractive index of 1.46 and clad refractive index 1.4595 with effective refractive index 1.4682 at 1550nm. An optical microscope type OLYMPUS, Measuring Microscope STM-UM was used to measure the dimensions of the optical fiber as shown in Figure 4. The fiber core radius is $4.59\mu m$. The cladding radius is about $62\mu m$. The fiber core is at a distance of $3\mu m$ from the flat surface of the fiber.

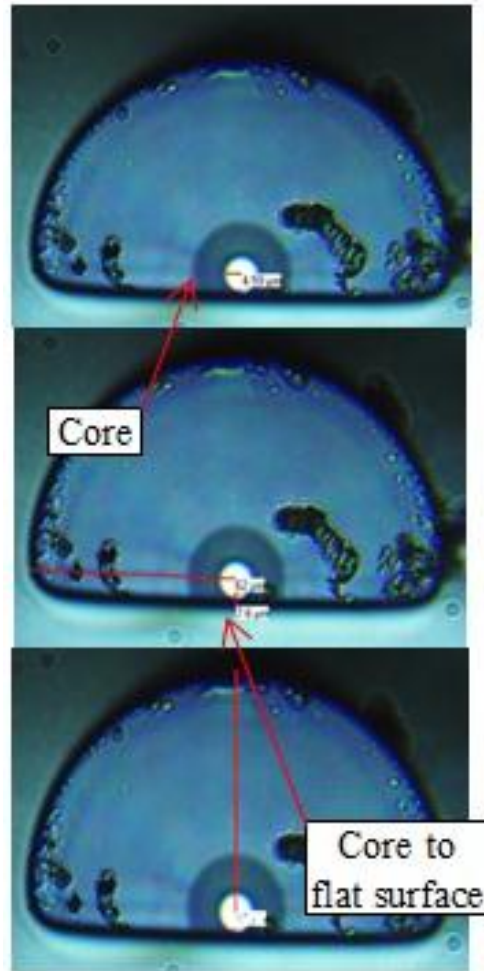


Fig. (4): Microscopic image of a D-Shaped fiber showing the dimensions under NeoDPlan IC 20, $f=180mm$.

The fiber was dipped in a hydrogen gas chamber at 2400 psi for two weeks to increase its photosensitivity to UV laser light.

Second stage: writing the Bragg grating into the fiber core,

The Bragg grating was written on the optical fiber by a phase mask method using a UV Excimer Laser source. The laser source is of type GSI Lumonics Pulse Master Laser PM-844 model with 450mJ as a maximum energy. This laser emits in the UV region at 248nm and has a repetition rate of 50 Hz. The average power is about 20W. The pulse duration can be varied from 12ns to 20ns giving peak power of 22.5MW at 20ns. The voltage supply provides voltages up to 40KV. The laser parameters that were employed to write the FBG in our experimental work are 50 mJ/cm² pulse fluence at 20 pulse/sec repetition rate for 3.5 min. The pulse fluence is 50mJ/cm²,

$$\text{Total cumulative fluence} = 3.5 \times 60 (\text{sec}) \times 20(\text{RR}) \times \frac{50\text{mJ}}{\text{cm}^2} = \frac{0.21\text{KJ}}{\text{cm}^2}$$

The first step in operating this laser system is to turn on the cooling system before turning gradually the voltage supply up to 27KV. The gas pressure inside the cavity is about 4500mbar. The fiber is connected from one of its end to an optical spectrum analyzer OSA type Agilent 86140 series and broadband light source type MPB EBS-7210 via an optical circulator for monitoring the reflectivity during fabrication. The fiber is clamped by a fiber holder in front of the phase mask and the spacing between them is monitored by a CCD camera mounted overhead and adjusted by a motion stage with 6 axis adjustments. Figure 5 shows a schematic diagram of this setup.

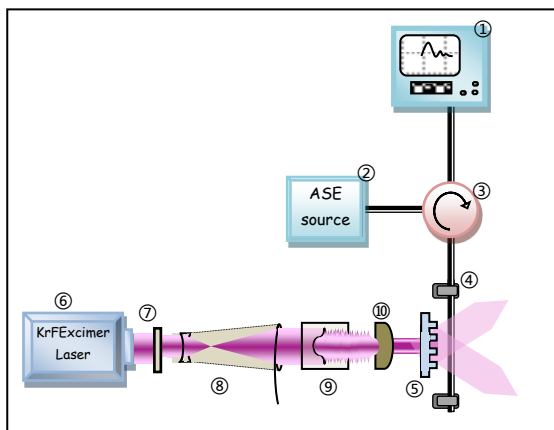


Fig.(5): Fiber Bragg Grating phase mask fabrication setup, ① OSA, ② broadband light source, ③ optical circulator, ④ clamber, ⑤ phase mask, ⑥ KrFexcimer laser, ⑦ rectangular aperture, ⑧ beam expander, ⑨ apodization mask, ⑩ cylindrical lens.

The KrFexcimerlaser is switched on then the UV output light beam is shaped by a rectangular aperture of 1cm×0.5cm dimensions and homogenized by a beam expander, apodization mask and a cylindrical lens to get a good focus with normal incidence UV light beam on the phase mask. The phase mask has a length of 4 cm and a grating period about 1057 nm. An interference pattern between modes (m= +1) and (m=-1) where m represents the mode number, is created on the fiber and it is monitored by a white paper on a screen in front of the fiber. The reflectivity is monitored on the OSA where when it reaches its highest value at -30 dBm then the excimer laser is switched off.

Results

Based on coupled mode theory which is implemented using appropriately structured MATLAB program. The grating period is deduced to be 5.2786*10⁻⁰⁷ m (527.86 nm) with Bragg wavelength at 1550nm. The reflectivity at this period is close to unity as shown in Figure 6. Effective phase mask period for writing the desired fiber Bragg Grating on our D-Shaped single mode fiber is supposed to be twice the latter value giving the value of 1055.7nm (Eq. 11).

Among the available physical phase mask was one with 1057 nm period. Throughout all the written fiber Bragg gratings this 1057nm phase mask was used in the experiment. The resultant calculated reflectivity (Eq. 9) for this phase mask period is shown in Figure 7.

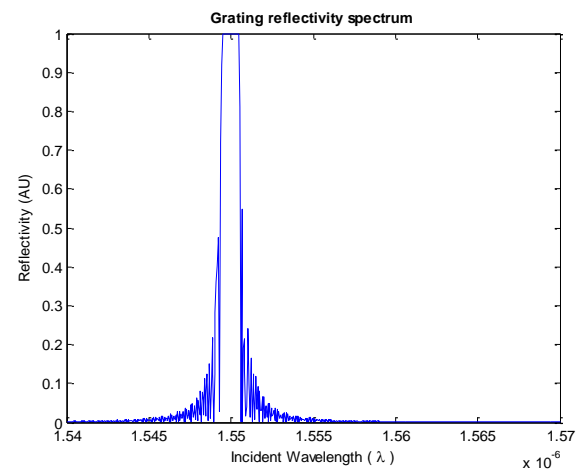


Fig. (6): The reflectivity spectrum of the fiber Bragg grating due to the phase mask of 1055.7nm period and the resultant Bragg wavelength is 1550 nm.

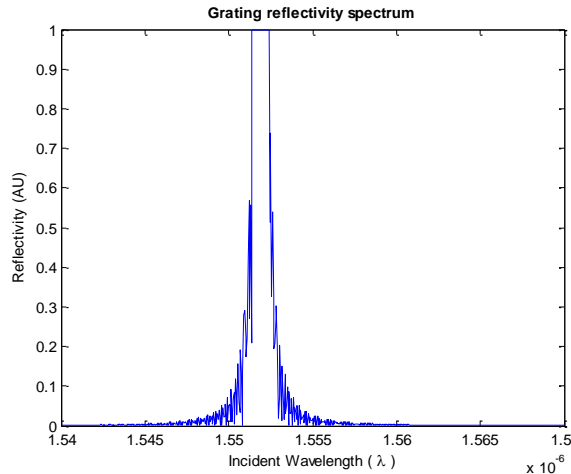


Fig. (7): The reflectivity spectrum of the fiber Bragg grating due to the phase mask of 1057nm period and the resultant Bragg wavelength is 1551.9nm.

It is clear from Figure 7 there is a slight shift in the reflectivity spectrum due to the 1.4nm difference in the phase mask which results in a wavelength shift of 6.3nm.

Experimentally, the Bragg grating is written for 3.5 min on a D-shaped optical fiber. The reflection spectrum is recorded as shown in Figure 8.

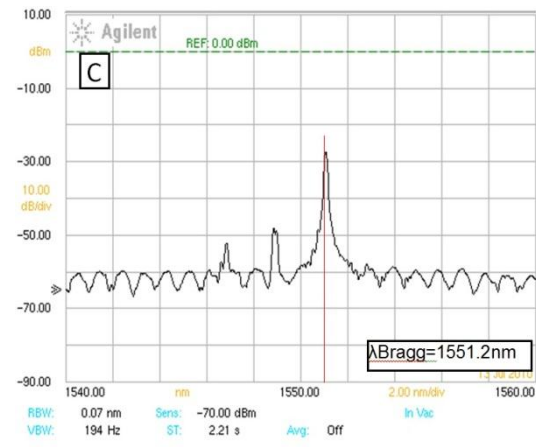
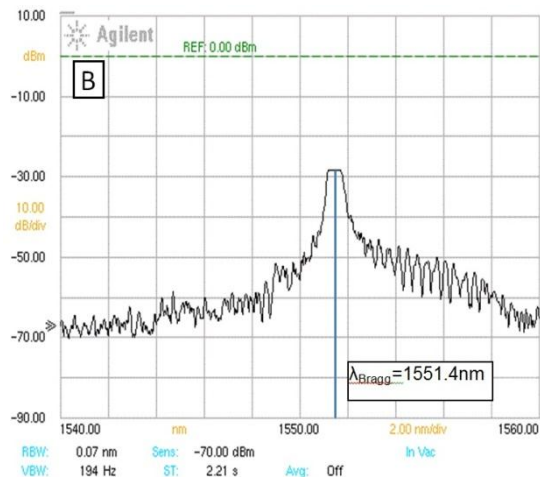
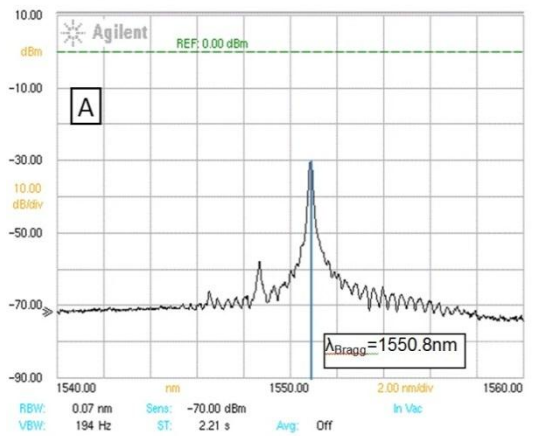


Fig. (8): The reflectivity spectrum in dBm units as a function of incident light wavelength recorded by OSA, A; $\lambda_{Bragg}=1550.8\text{nm}$, B; $\lambda_{Bragg}=1551.4\text{nm}$, and C; $\lambda_{Bragg}=1551.2\text{nm}$.

Figure 8 (A B and C) shows the reflectivity spectrum in dBm units as a function of incident light wavelength. The three manufactured fiber Bragg grating were made under the same conditions except one factor. This factor was related to the direct facing of the D-shape geometry to the phase mask which was done manually. In general, we would expect that the best results are obtained when the alignment is optimum meaning that the tip of the D geometry is located opposite to the phase mask directly. The criterion of the best fiber Bragg grating is the one which gives stable and flat reflectivity over relatively a wide range. In our case, fiber Bragg grating of C gave the best performance as it obvious from the reflectivity spectrum.

So the difference in the Bragg wavelength of the calculated value Figure 7 and experimental value Figure 8,C is 0.7nm. The error rate is 0.045 % which is considered very low and acceptable.



Conclusion

Positioning the core of the D-shaped single mode optical fiber as much as possible in front of the phase mask leads to efficient fiber Bragg grating regarding reflectivity.

References

- [1] Y J. Rao, D.J.Webb, D.A. Jackson, L. Zhang, and I. Benrriou, Optical in Fiber Bragg Grating Sensor System for Medical

- Applications, Journal of Biomedical Optics, 3(1), 33-44, (1998).
- [2] Nahar Singh, Subhash C Jain, A K Aggarwal and R P Bajpai, Fiber Bragg Grating writing using Phase Mask Technology, Journal of Scientific and Industrial Research, 64, 108-115, (2005).
- [3] K.O.Hill, Y. Fujii, D. C. Johnson, and B. S. Kawasaki, Photo-sensitivity in optical fiber waveguides: application to reflection filter fabrication, Applied Physics Letters, 32, 647-649, (1978).
- [4] Swanton A., Armes D. J., Young-Smith K. J., Dix C., and Kashyap R., Use of e-beam written, reactive ion etched, phase masks for the generation of novel photorefractive, special Issue, Journal of Micro. Electronics Engineering, 30, 509-512, 1996.
- [5] Lemaire P.J., Atkins R. M., Mizrahi V., and Reed W. A., High Pressure H₂-Loading As A Technique For Achieving Ultra High UV Photosensitivity And Thermal Sensitivity In Ge₂ Doped Optical Fibers, Electronics Letters, Vol. 29, 1191-1193, (1993).
- [6] Chen T., Fiber Optic Sensors for Extreme Environments, PhD Thesis submitted to the Graduate Faculty of Swanson School of Engineering, University of Pittsburgh, (2012).
- [7] K. Zhou, X. Chen, L. Zhang, and I. Bennion, High-sensitivity optical chemosensor based on etched D-fiber Bragg gratings, Electronics Letters, 40, 232-234, (2004).
- [8] Jia- Minglin, Photonic Devices, Cambridge University Press, 2005.
- [9] Raman, Fiber Bragg Gratings, Science Direct, (2010).

كتابة محرز الحيود نوع براغ على الليف البصري شكل حرف D باستخدام ليزر الإكسايمر نوع فلوريد الكربتون

شيماء رياض محمد علي⁽¹⁾ خليل ابراهيم حاجم⁽¹⁾ رونك زاتك جن⁽²⁾ كفن بينك جن⁽²⁾

(1) معهد الليزر للدراسات العليا، جامعة بغداد، بغداد، العراق
(2) قسم هندسة الكهرباء والحاسوب، مدرسة سوانسن للهندسة، جامعة بتسبرغ، بتسبرك، بنسلفانيا، الولايات المتحدة الأمريكية

الخلاصة: لليف الضوئي ذو محرز الحيود نوع براك عدة فوائد حيث من الممكن استخدامه كمتحسس حراري او متحسس للضغط او حتى متحسس لمعامل الانكسار. عملية تصميم كل نوع من هذه المتحسسات تتضمن بعض المتطلبات. إن متحسس معامل الانكسار المصنوع من الليف الضوئي ذو محرز الحيود نوع براغ تطبيق مهم جداً. توجد طرق متعددة من اجل زيادة قابلية التحسس لهذا النوع من الليف الضوئي ذو محرز الحيود من نوع براغ. في عملنا المقترح، تمت كتابة محرز الحيود نوع براغ في ليف ضوئي احادي النمط (مقطعه العرضي على شكل حرف D) بأتباع تقنية القناع الطوري باستخدام ليزر الأكسايمر -الكربتون فلورايد. واطهر محرز الحيود نوع براغ و الذي تم تصنيعه في الليف الضوئي قابلية انعكاس عالية تصل الى نسبة 99,99% وبطول موجة براغ يصل الى 1551,2 نانومتر لتكون أفضل نتيجة يمكن الحصول عليها من القناع الطوري ذات طول مشبكي يقدر بـ 1057 نانومتر. تم التوصل الى ان تدوير القلب لليف الضوئي باتجاه القناع الطوري دور مهم جداً في تحديد كفاءة العمل لليف الضوئي لمحزر الحيود نوع براغ المصنع.